

## SWELLING-INDUCED INSTABILITY OF SUBSTRATE-ATTACHED HYDROGEL LINES

MIN KYOO KANG and RUI HUANG\*

*Department of Aerospace Engineering and Engineering Mechanics  
University of Texas, Austin, TX 78712, USA*

*\*[ruihuang@mail.utexas.edu](mailto:ruihuang@mail.utexas.edu)*

Received 1 September 2010

Accepted 27 October 2010

Micro- and nano-scale hydrogel lines can be fabricated on substrates by top-down approaches such as lithography and micro/nano-imprint. When in contact with a solvent, the hydrogel lines swell under the constraint of the substrate, often resulting in distorted shapes or instability patterns. In this paper, using a nonlinear finite element method, the effects of material and geometry on swell-induced instability of substrate-attached hydrogel lines are studied. Firstly, with a two-dimensional plane-strain model, we show that crease-like surface instability occurs in hydrogel lines with the width-to-height aspect ratio greater than a critical value. Next, for relative low aspect ratios, we show that a global buckling instability occurs. In both cases, the critical conditions depend on the material parameters that characterize the elastic stiffness of the polymer network and the chemical interaction between solvent and polymer in the hydrogel.

*Keywords:* Hydrogel; buckling; creasing; soft matter.

### 1. Introduction

Hydrogel-based soft materials have been demonstrated for a large variety of applications, including sensors and actuators [Beebe *et al.*, 2000; Sidorenko *et al.*, 2007], drug delivery [Jeong *et al.*, 1997; Qiu and Park, 2001], and bioengineering [Galaev and Mattiasson, 1999; Peppas *et al.*, 2006; Ulijn *et al.*, 2007; Tokarev and Minko, 2009]. Experimental studies have shown complex material behaviors of gels. In particular, when subject to geometric confinement and/or mechanical constraint, a variety of deformation instability patterns have been observed in gel-like materials [Southern and Thomas, 1965; Tanaka *et al.*, 1987, 1992; Mora and Boudaoud, 2006; Trujillo *et al.*, 2008; Sultan and Boudaoud, 2008; Guvendiren *et al.*, 2009, 2010].

Recently, micro- and nano-scale hydrogel lines and particles have been fabricated using top-down approaches such as lithography and nano-imprint [Tirumala *et al.*, 2005; DuPont *et al.*, 2010; Glangchai *et al.*, 2008]. During the fabrication process, these lines may be immersed in a solvent and swell. As the lines are typically

\*Corresponding author.

attached to a rigid substrate on one side, swelling deformation is often inhomogeneous and anisotropic due to the effect of substrate constraint. Global buckling as well as local instability patterns has been observed [Tirumala *et al.*, 2005; DuPont *et al.*, 2010]. However, the critical condition for swell-induced instability of such hydrogel line structures has not been fully understood. In this paper, by using a recently developed nonlinear finite element method [Kang and Huang, 2010a], we show that two types of instability patterns can occur in hydrogel lines, depending on the material and geometry.

This paper is organized as follows. Section 2 presents a brief introduction to the fabrication process and observation of hydrogel lines. Section 3 introduces the nonlinear finite element method. In Sec. 4, two-dimensional finite element analysis is performed for hydrogel lines with various width-to-height aspect ratios, showing crease-like surface instability. In Sec. 5, three-dimensional finite element analysis shows global buckling of hydrogel lines, depending on the aspect ratio and hydrogel material parameters. Section 6 summarizes the present study.

## 2. Fabrication and Observation

To put the theoretical study in perspective, a brief introduction to a top-down fabrication process and experimental observation of micro/nano-scale hydrogel lines is presented here, following Tirumala *et al.* [2005]. A similar process was used by DuPont *et al.* [2010], while an alternative approach was developed by Glangchai *et al.* [2008]. As shown in Fig. 1, a polymer solution was first spin-coated onto a silicon wafer, with the film thickness ranging from 30 to 250 nm. The polymer

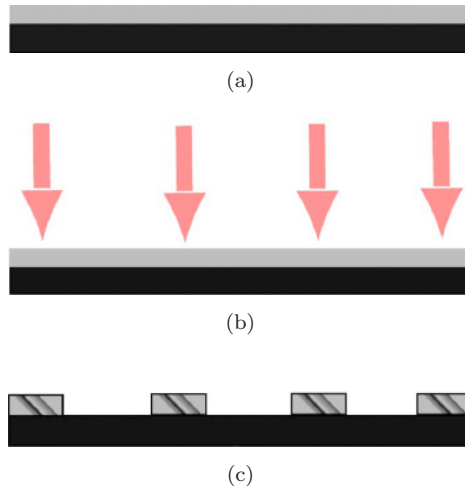


Fig. 1. Schematic of a fabrication process of hydrogel lines: (a) spin-coat, (b) electron-beam exposure, (c) development in water (Adopted from Tirumala *et al.*, 2005).

film was then patterned by a direct-write electron-beam lithography technique. Electro-beam irradiation has been routinely used to crosslink bulk polymers. By using a focused electron-beam system, the exposed region of the polymer thin film was crosslinked while the non-irradiated regions remain uncrosslinked. Subsequently, the uncrosslinked polymer was dissolved in water, leaving behind the crosslinked polymer lines. The crosslink density ( $\rho_c$ ) can be tuned by varying the dwelling time of electron-beam exposure. The polymer lines were then immersed in water until they were fully swollen. For the purpose of observation, the swollen lines were flash-dried using a nitrogen gun to preserve the morphology.

Figure 2 shows a set of swollen polymer nano-lines, which were designed to study the effect of line width on swell-induced buckling. It was found that both the buckling wavelength and amplitude scale linearly with the line width. In addition, the buckling amplitude decreases with increasing crosslink density ( $\rho_c$ ), while the buckling wavelength is independent of the crosslink density ( $\rho_c$ ). However, the critical condition for swell-induced buckling was not established experimentally, and the selection of a particular buckle wavelength was not well understood either.

A similar buckling instability was also observed in a thin strip of soft gel clamped to a stiff gel by Mora and Boudaoud [2006], who also conducted a linear perturbation analysis using the thin-plate equations of linear elasticity. An important result of their theoretical analysis is the prediction of the buckle wavelength to scale linearly with the width of the strip. However, it was found that this prediction in general does not apply for hydrogel lines [DuPont *et al.*, 2010; Liu *et al.*, 2010]. Firstly, the swelling behavior of the hydrogel is typically nonlinear and cannot be described sufficiently by linear elasticity. Secondly, the geometry of the hydrogel lines, with the width-to-height aspect ratio around 1 or larger, cannot be simply modeled as thin plates. For these reasons, we perform numerical simulations based on a nonlinear finite element method to study swell-induced instability in hydrogel lines.

Image not available. Permission pending.

Fig. 2. Atomic force micrographs of swollen polymer lines. The dry-state width:height dimensions are labeled in each panel, and the lines were  $5\ \mu\text{m}$  long before swelling (Tirumala *et al.*, unpublished).

### 3. A Nonlinear Finite Element Method

A theoretical framework for swelling deformation of hydrogels has been developed [Hong *et al.*, 2008, 2009a], based on which a nonlinear finite element method has been implemented to simulate inhomogeneous swelling of hydrogels under various constraints [Kang and Huang, 2010a]. Within a commercial finite element package [ABAQUS, 2008], the hydrogel is modeled as a hyperelastic material with the constitutive behavior described by a user subroutine (UMAT). Briefly, the specific material model is based on a free energy function that consists of elastic free energy of the polymer network and the free energy of mixing the solvent molecules with the polymer chains [Flory, 1953]. For equilibrium analyses, the chemical potential in the hydrogel is a constant and mimicked by a temperature-like quantity in the user subroutine. In terms of the deformation gradient and the chemical potential, the free energy density function for a hydrogel takes the form of:

$$\begin{aligned} \hat{U}(\mathbf{F}, \mu) = & \frac{1}{2} N k_B T (I - 3 - 2 \ln J) \\ & + \frac{k_B T}{\nu} \left[ (J - 1) \ln \frac{J - 1}{J} + \chi \frac{J - 1}{J} \right] - \frac{\mu}{\nu} (J - 1), \end{aligned} \quad (1)$$

where  $\mu$  is the chemical potential,  $\mathbf{F}$  is the deformation gradient tensor,  $I = F_{iK} F_{iK}$ ,  $J = \det(\mathbf{F})$ ,  $N$  is the effective number of polymer chains per unit volume,  $\chi$  is the Flory interaction parameter,  $\nu$  is the volume per solvent molecule,  $T$  is the absolute temperature, and  $k_B$  is the Boltzmann constant. Thus, the material properties of the hydrogel is fully determined by three parameters:  $Nk_B T$ ,  $k_B T/\nu$ , and  $\chi$ . The first two combine to give one dimensionless parameter,  $N\nu$ . It is well known that  $Nk_B T$  defines the initial shear modulus of the polymer network, with the number  $N$  proportional to the crosslink density ( $\rho_c$ ) [Treloar, 1975].

Based on Eq. (1), the explicit formula for the true stress and tangent modulus were derived, and a user material subroutine was coded in the format of ABAQUS/UMAT [Kang and Huang, 2010a]. With such, the standard finite element method for hyperelastic materials can be used to simulate swelling behavior of hydrogels under various constraints, as the mathematical formula (including boundary conditions) is identical except for the free energy function. Both two-dimensional (2D) and three-dimensional (3D) simulations can be conducted, with appropriate boundary conditions for specific problems. We emphasize that the present study considers equilibrium swelling only. The detailed mathematical formula and numerical implementation has been presented in a previous study [Kang and Huang, 2010a].

### 4. Two-Dimensional Simulations: Creasing

In this section, we model 2D plane-strain swelling of the hydrogel lines, assuming infinitely long lines and no global buckling. The 2D simulations serve two purposes. Firstly, they provide solutions for swollen hydrogel lines without buckling, which offer insights into the critical condition for buckling. Second, they illustrate

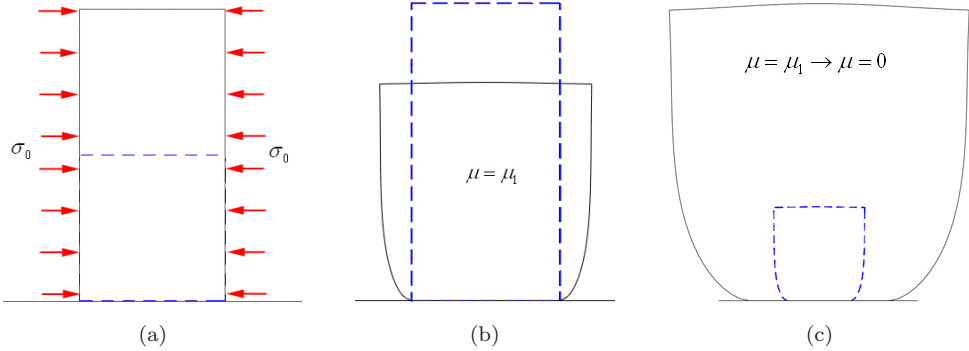


Fig. 3. Illustration of the two-step finite element analysis (FEA): (a) the initial state ( $\mu = \mu_1$ ), homogeneously swollen with side pressure; (b) FEA Step 1, releasing the side pressure; (c) FEA Step 2: swelling up to the equilibrium chemical potential ( $\mu = 0$ ).

creasing instability in wide lines. Each line has a rectangular cross section at the dry state, with one of the side faces bonded to the rigid substrate, as shown in Fig. 3(a). The bonding imposes a constraint on the swelling of the line, and the effect of the constraint varies with the width-to-height aspect ratio ( $W/H$ ). Swelling deformation of such a substrate-attached hydrogel line is typically inhomogeneous, with two homogeneous limits: (i) When  $W/H \rightarrow \infty$ , the line becomes a film, with homogeneous swelling in the thickness direction only; (ii) When  $W/H \rightarrow 0$ , the lateral constraint by the substrate becomes negligible, and the swelling becomes homogeneous and laterally isotropic. The solutions for the two homogeneous limits have been obtained analytically in the previous study [Kang and Huang, 2010a], which set the upper and lower bounds for the volume swelling ratio of the hydrogel lines.

Following Kang and Huang [2010a], a two-step finite element analysis was performed to simulate the inhomogeneous swelling of the hydrogel lines, as illustrated in Fig. 3. We start from an anisotropic initial state of homogeneous swelling with an arbitrarily selected swelling ratio in the height direction of the line, as shown in Fig. 3(a). Such an initial state is identical to that for homogeneous swelling of a hydrogel thin film, for which the chemical potential can be analytically obtained as a function of the swelling ratio. However, a compressive stress (or pressure) has to be applied to the side faces of the line to maintain the homogeneous swelling, which apparently violates the traction-free (natural) boundary condition of the intended problem. To recover the traction-free boundary condition, we release the side pressure gradually during the first step of numerical simulation, while keeping the chemical potential in the hydrogel unchanged. As shown in Fig. 3(b), the release of the side pressure leads to an inhomogeneous deformation of the hydrogel line at the initial chemical potential ( $\mu = \mu_1$ ). This step is necessary because a finite chemical potential ( $\mu_1 < 0$ ) has to be numerically specified at the initial state. Subsequently, further swelling of the hydrogel line is simulated by increasing the chemical potential until  $\mu = 0$ , as shown in Fig. 3(c). Here, the chemical potential

serves as a loading parameter, analogous to temperature for thermally induced deformation.

A relatively fine finite element mesh is required for simulating inhomogeneous swelling deformation, especially at locations such as the lower corners where a high strain gradient is expected. For each model in the present study, the finite element mesh is refined until the result converges satisfactorily. The total number of elements depends on the aspect ratio and the material parameters, and the convergence of the numerical results is justified by the volume swelling ratio with a tolerance of  $10^{-3}$ . The bonding of the bottom face of the hydrogel line to the rigid substrate is mimicked by applying a zero-displacement (essential) boundary condition; debonding of the line is not considered in the present study. Furthermore, the large deformation due to swelling often results in contact of the side faces of the hydrogel line with the substrate surface, for which hard and frictionless contact properties are assumed in the numerical simulations.

The inhomogeneous swelling deformation at the equilibrium chemical potential ( $\mu = 0$ ) is plotted in Fig. 4 for three hydrogel lines with  $W/H = 1, 10,$  and  $12$ . The dimensionless material parameters of the hydrogel,  $N\nu$  and  $\chi$ , are set to be  $0.001$  and  $0.1$ , respectively. These parameters are within the range of realistic materials [Flory, 1953; Treloar, 1975], but they are chosen arbitrarily here for illustrative purpose with no specific materials in mind. For each line, the cross section at the dry state is outlined by a small rectangular box. The large swelling deformation pushes the side faces of the hydrogel lines to form contact with the rigid substrate surface. The contact length increases as the aspect ratio increases, reaching a full contact of the side faces for the hydrogel line with  $W/H = 10$ . The stress contours show stress concentration at the bottom corners, where debonding may occur. Note that the magnitude of the stress in Fig. 4 is normalized by  $Nk_B T$ , which is typically in the range of  $10^4 \sim 10^7$  Pa for polymeric hydrogels at the room temperature [Trujillo *et al.*, 2008].

As the aspect ratio  $W/H$  increases beyond  $10$ , swelling deformation of the hydrogel line induces an increasingly large compressive stress at the top surface. It is found that, at a critical aspect ratio, a local surface instability occurs, as shown in Fig. 4(c) for  $W/H = 12$ . In this case, as the chemical potential increases, the top surface of the hydrogel line evolves from nearly flat to slightly undulated, and eventually forms crease-like folding with self-contact. More creases are observed in the simulation for a hydrogel line with the aspect ratio  $W/H = 13$ . However, the numerical simulation becomes increasingly unstable with formation of the surface creases, possibly due to the singularity at the tip of each crease. Numerical stabilization can be used to prevent divergence in search of the numerical solutions. However, it remains a numerical challenge to be addressed for simulations of hydrogel lines with higher aspect ratios. It is worth mentioning that the surface creases form automatically in the present numerical simulations for hydrogel lines beyond the critical aspect ratio, without a need to introduce any perturbation. We speculate that the instability is

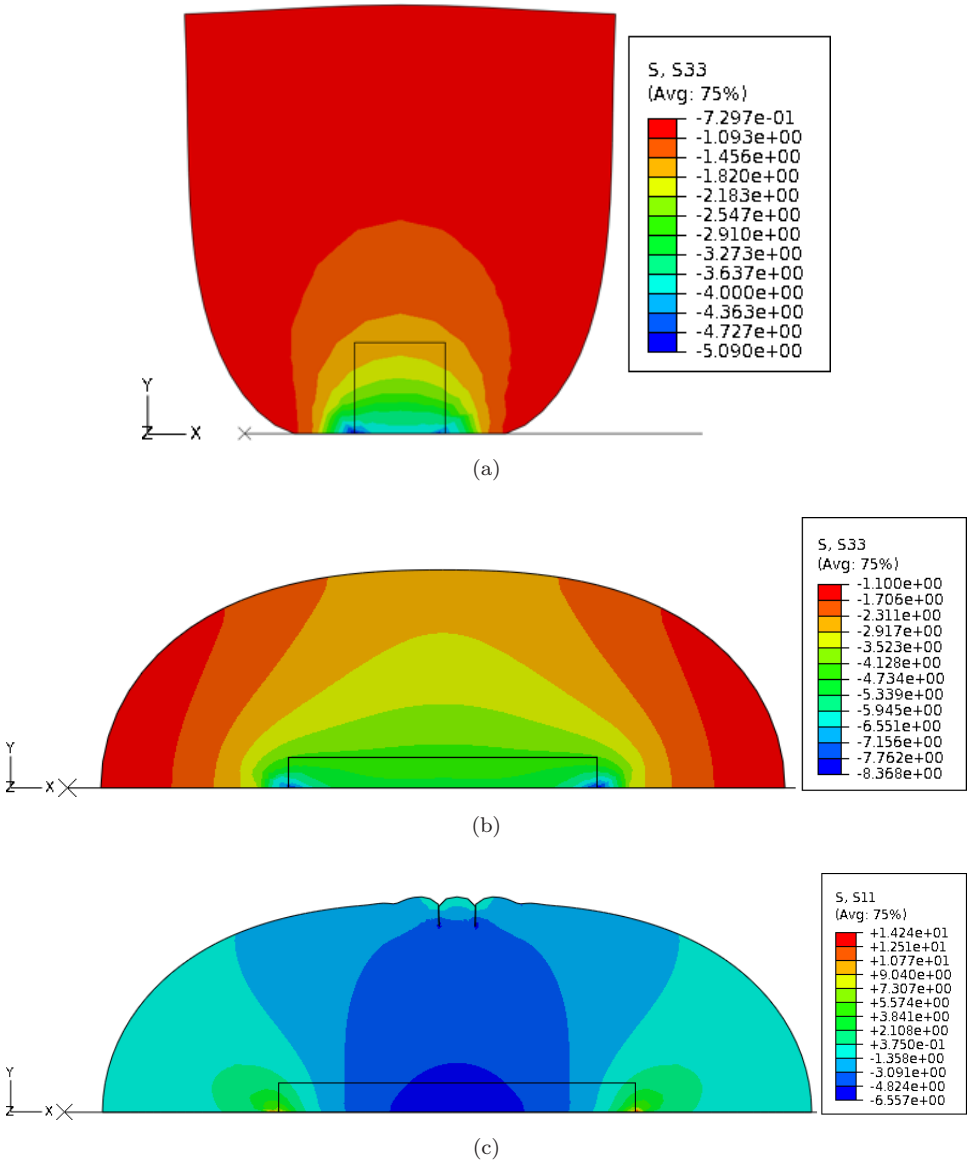


Fig. 4. Effect of the width-to-height aspect ratio on two-dimensional swelling of hydrogel lines. (a)  $W/H = 1$ ; (b)  $W/H = 10$ ; (c)  $W/H = 12$ . The rectangular boxes outline the cross sections at the dry state.

triggered by numerical fluctuations associated with the inhomogeneous deformation of the hydrogel even without surface creases. It is also noted that the contact of the side faces of the hydrogel line with the substrate surface plays an important role giving rise to the compressive stresses in the hydrogel. In simulations without

enforcing this contact, the hydrogel line swelled more significantly and wrapped around the bottom surface, while surface creases were not observed.

Formation of surface creases has been observed experimentally in swelling gels [Southern and Thomas, 1965; Tanaka *et al.*, 1987, 1992; Trujillo *et al.*, 2008; Guvendiren *et al.*, 2009, 2010]. A wide range of critical swelling ratios were reported for different gel systems, between 2.46 and 3.72 by Tanaka *et al.* [1992] and around 2 by Trujillo *et al.* [2008]. In an experimental study of surface-attached hydrogel thin films, Trujillo *et al.* [2008] found that the critical condition for surface creasing in their experiments agreed well with the prediction by a linear perturbation analysis for rubber under equi-biaxial compression [Biot, 1963], with a critical linear compressive strain  $\sim 33\%$  relative to the state of free swelling for unconstrained hydrogels. On the other hand, Gent and Cho [1999] found that Biot's prediction considerably overestimated the critical strain for surface creasing in their experiments with rubbers compressed by mechanical bending. More recently, Hong *et al.* [2009b] suggested that surface creasing is a different mode of surface instability in contrast with Biot's linear perturbation analysis, and they predicted a critical swelling ratio at 2.4 for surface creasing of gels based on an energetic consideration and numerical calculations for neo-Hookean elastomers. In a previous study [Kang and Huang, 2010b], we extended Biot's linear perturbation analysis to swelling deformation of a substrate-confined hydrogel layer and predicted a material specific critical condition for surface instability, with the critical swelling ratio ranging from about 2.5 to 3.4, depending on the material parameters of the hydrogel. Further, we showed that the effect of surface tension leads to a thickness-dependent critical condition and a finite characteristic wavelength [Kang and Huang, 2010c].

For the surface-attached hydrogel lines in the present study, we suggest a similar critical condition for creasing, with an additional effect due to the geometry. Our numerical simulations show that the critical aspect ratio for the onset of surface instability depends on the two dimensionless material parameters of the hydrogel, that is:

$$(W/H)_c = f_1(N\nu, \chi), \quad (2)$$

which is approximately 12 for  $N\nu = 0.001$  and  $\chi = 0.1$ . The critical aspect ratio increases as  $N\nu$  or  $\chi$  increases. At a limiting case when  $(W/H)_c \rightarrow \infty$ , the hydrogel is stable in all aspect ratios including the case of a blanket film.

## 5. Three-Dimensional Simulations: Buckling

To study swelling induced buckling of the hydrogel lines, 3D simulations are performed and discussed in this section. Figure 5 shows a 3D finite element model for a hydrogel line. The eight-node brick elements (C3D8) in ABAQUS are used for the hydrogel, while the substrate is modeled as a rigid surface. The bottom surface of the hydrogel is fixed, assuming no debonding from the substrate. Symmetric boundary conditions are applied at both ends of the line along the longitudinal



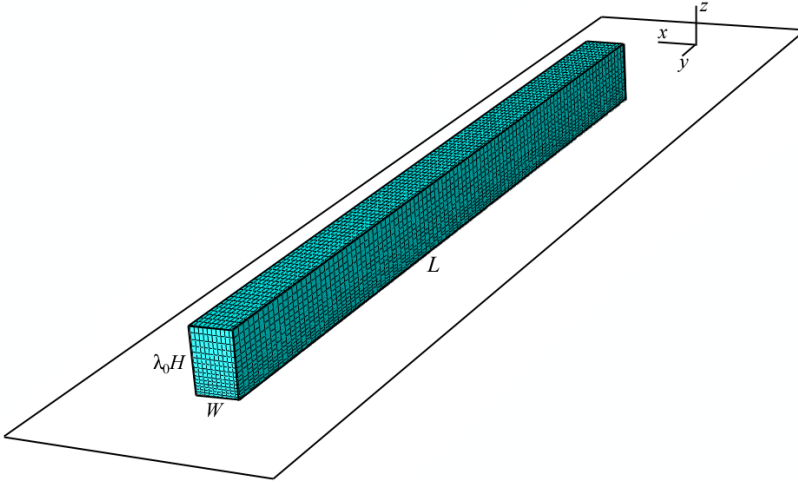


Fig. 5. A three-dimensional finite element model of a hydrogel line attached to a rigid substrate, with an initial swelling ratio  $\lambda_0$  in the thickness direction.

direction to eliminate the end effect and mimic an infinitely long line. The length  $L$  is arbitrarily selected to be several times of the buckle wavelength. The top and side faces of the hydrogel line are traction-free. Contact between the side faces and the substrate is defined as well as possible self-contact of the free surfaces.

The simulation procedure is similar to that for the 2D model as illustrated in Fig. 3. First, a homogeneous initial state is determined from the analytical solution for the 1D swelling in the thickness direction, with an arbitrary initial swelling ratio ( $\lambda_0$ ) at a finite chemical potential ( $\mu_1 < 0$ ). Such an initial state comes with an initial pressure acting on the side faces. To recover the traction-free boundary condition, the side pressure is released during the first numerical step, while the chemical potential is kept constant. Next, the simulation continues by increasing the chemical potential (as a loading parameter) till the equilibrium state ( $\mu = 0$ ). To numerically trigger the buckling instability, a periodic imperfection of small amplitude is introduced by a cubic spline curve in the longitudinal direction of the hydrogel line. The spline curve is generated automatically by ABAQUS, defined piecewise by a polynomial function. For the present study, a cubic spline curve of amplitude  $0.001H$  is used for each buckle wavelength.

To illustrate the effects of material properties and geometry on swell-induced buckling, two sets of numerical simulations are performed. Firstly, with the identical line geometry, the material parameter ( $N\nu$ ) is varied. All parameters are chosen arbitrarily for the purpose of illustration, but they are within the range of realistic materials. Figure 6 shows the equilibrium swollen shapes for a set of hydrogel lines with  $W/H = 1$  and  $\chi = 0.55$ . For  $N\nu = 0.1$ , the hydrogel is relatively stiff, with a low degree of swelling. As a result, the hydrogel line remains essentially straight, with no buckling. As  $N\nu$  decreases, the hydrogel becomes softer and the degree of

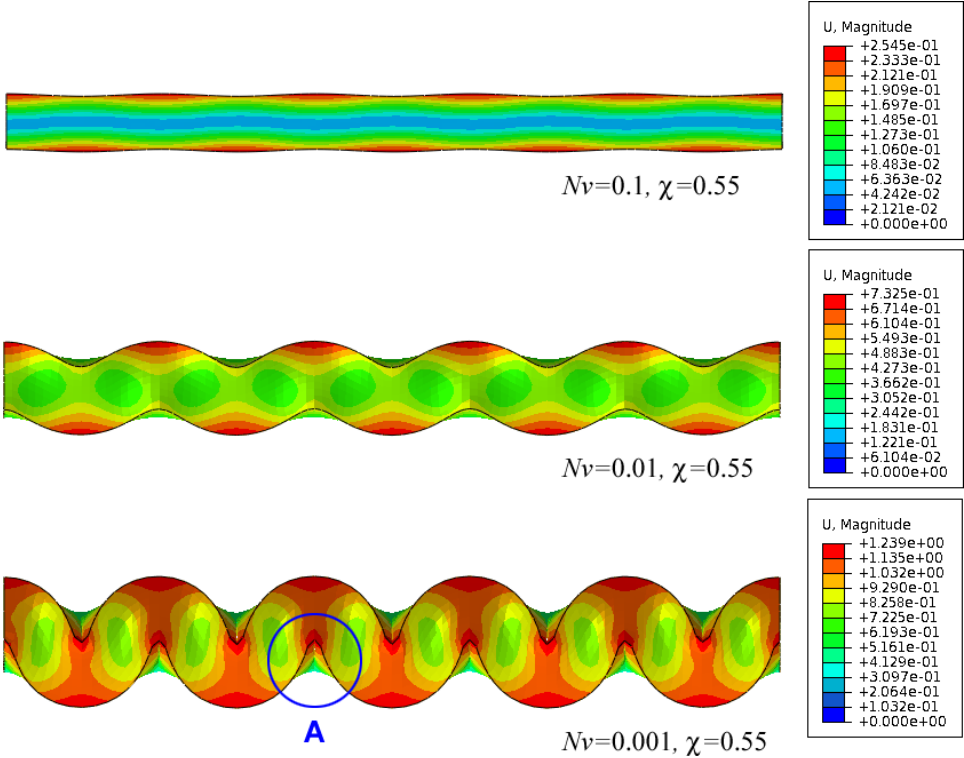


Fig. 6. Swell-induced buckling of hydrogel lines bonded to a rigid substrate, with different  $N\nu$  and  $W/H = 1$ . The circle A indicates a location with self-contact of the side face due to buckling.

swelling increases. For  $N\nu = 0.01$  and  $0.001$ , the hydrogel lines become buckled upon swelling. Note that the buckling wavelength ( $S$ ) in these simulations is arbitrarily set by the initial imperfection, which is four times the height ( $H$ ). The physical criterion for the wavelength selection has not been established theoretically. Nevertheless, the present simulations show increasing buckle amplitude with decreasing  $N\nu$ , in qualitative agreement with the experiments [Tirumala *et al.*, 2005]. Figure 7 plots the buckling amplitude as a function of  $N\nu$ . As  $N\nu$  decreases, the buckling amplitude increases rapidly at a certain value of  $N\nu$ , from which a critical value of  $N\nu$  may be determined for swell-induced buckling of the hydrogel lines. By a dimensional consideration, the critical value may be written as a function of the buckle wavelength ( $S/H$ ), the aspect ratio ( $W/H$ ), and the parameter  $\chi$ , namely

$$(N\nu)_c = g_1(S/H, W/H, \chi). \tag{3}$$

Alternatively, for each hydrogel line, the buckling amplitude may be calculated as a function of the buckle wavelength, i.e.,

$$A/H = g_2(S/H; W/H, N\nu, \chi). \tag{4}$$

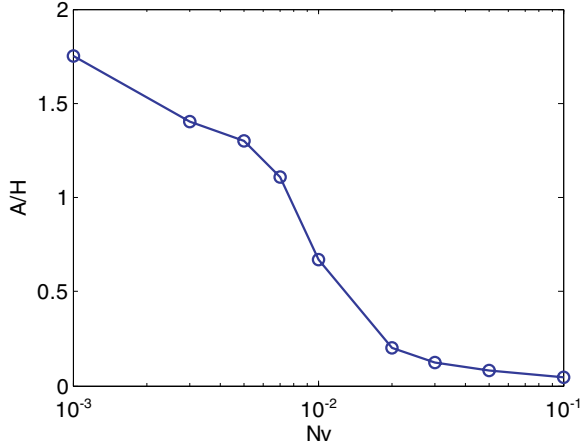


Fig. 7. Normalized buckling amplitude as a function of  $N\nu$ , for  $W/H = 1$  and  $\chi = 0.55$ .

A possible criterion for the wavelength selection may then be set up by maximizing the buckle amplitude. Such a criterion may be considered to be equivalent to maximizing the volume swelling ratio or to minimizing the free energy (or maximizing the entropy).

It is noted that, since the bottom surface of the hydrogel line is fixed, the swell-induced buckling deformation in general is more complicated than the classical Euler buckling of a column. While the top surface appears to buckle laterally in the in-plane direction, it is also highly twisted in the out-of-plane direction. Due to relatively large deformation, the cross section of the line is highly distorted. Consequently, the kinematics of deformation is much more sophisticated than simple bending. In addition, significant swelling may lead to contact between the side faces and the substrate surface, as shown in the 2D simulations (Fig. 4). Swell-induced buckling can also lead to self-contact of the side faces, as indicated by the circle in Fig. 6.

For the second set of simulations, the material properties of the hydrogel are fixed as  $N\nu = 0.01$  and  $\chi = 0.55$ , while the width-to-height aspect ratio ( $W/H$ ) of the line is varied. As shown in Fig. 8, the buckle amplitude decreases as the aspect ratio ( $W/H$ ) increases. For the case of  $W/H = 4$ , the line remains essentially straight with no buckling. The buckle amplitude as a function of the aspect ratio is plotted in Fig. 9. The buckle amplitude increases abruptly as the aspect ratio ( $W/H$ ) decreases, suggesting a critical aspect ratio of around 2. In general, the critical aspect ratio for swell-induced buckling may be determined as a function of the material properties as well as the buckle wavelength, namely

$$(W/H)_c = f_2(S/H, N\nu, \chi). \quad (5)$$

Recall that, in the two-dimensional model, there exists a critical aspect ratio for swell-induced creasing. Together, it may be speculated that swell-induced buckling

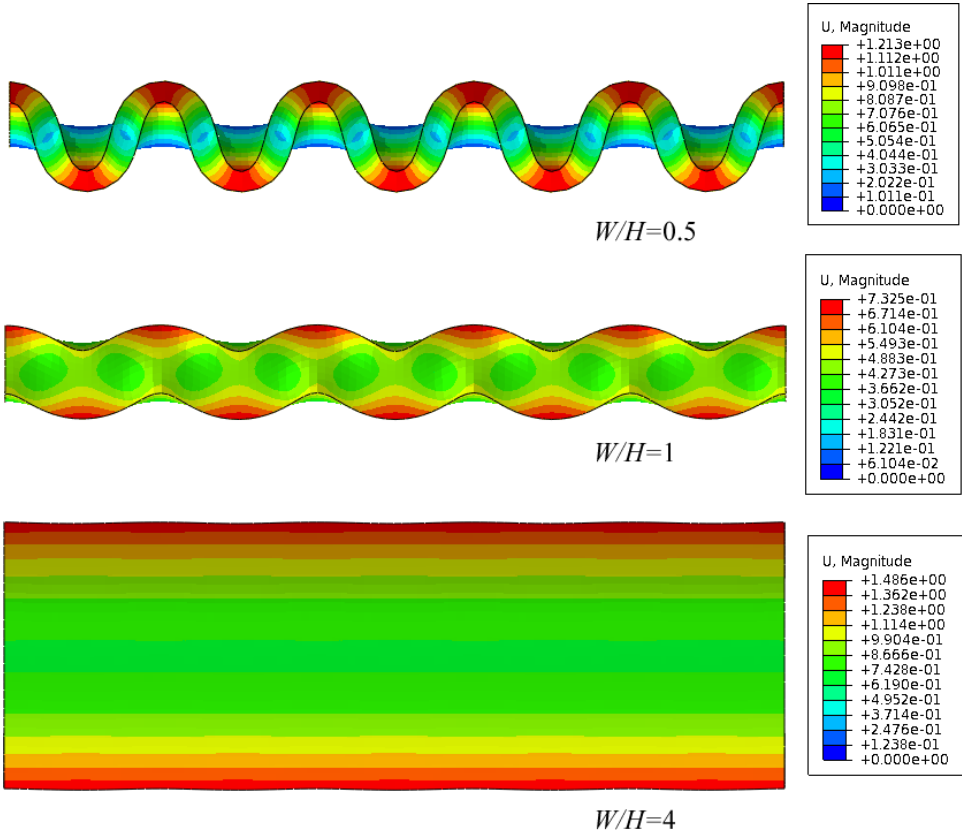


Fig. 8. Effect of the width-to-height ratio on swell-induced buckling of hydrogel lines bonded to a rigid substrate, where  $N\nu = 0.01$  and  $\chi = 0.55$ .

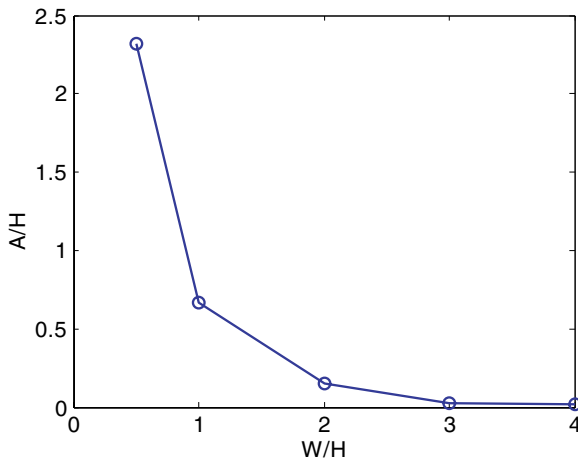


Fig. 9. Normalized buckling amplitude as a function of  $W/H$ , where  $N\nu = 0.01$ ,  $\chi = 0.55$ .

occurs for  $W/H$  less than a lower critical value (Eq. 5) and swell-induced creasing occurs for  $W/H$  greater than an upper critical value (Eq. 2). In between the two critical aspect ratios, the hydrogel line remains straight and stable. Both the lower and the upper critical aspect ratios depend on the material parameters ( $N\nu$  and  $\chi$ ) in general.

## 6. Summary

In this paper, a nonlinear finite element method is used to study the effects of material and geometry on swell-induced instability of substrate-attached hydrogel lines. Firstly, two-dimensional simulations show that crease-like surface instability occurs in hydrogel lines with the width-to-height aspect ratio greater than a critical value. Next, with three-dimensional models, we show that global buckling instability occurs in hydrogel lines with relatively small width-to-height ratios. In both cases, the critical conditions depend on the material parameters that characterize the elastic stiffness of the polymer network and the chemical interaction between solvent and polymer in the hydrogel.

## Acknowledgments

The authors gratefully acknowledge financial support by National Science Foundation through Grant No. 0547409.

## References

- ABAQUS (version 6.8), 2008. Dassault Systèmes Simulia Corp., Providence, RI, USA.
- Beebe, D. J., Moore, J. S., Bauer, J. M., Yu, Q., Liu, R. H., Devadoss, C. and Jo, B.-H. [2000] “Functional hydrogel structures for autonomous flow control inside microfluidic channels,” *Nature* **404**, 588–590.
- Biot, M. A. [1963] “Surface instability of rubber in compression,” *Appl. Sci. Res. A* **12**, 168–182.
- DuPont, S. J. Jr., Cates, R. S., Stroot, P. G. and Toomey, R. [2010] “Swelling-induced instabilities in microscale, surface-confined poly(N-isopropylacrylamide) hydrogels,” *Soft Matter* **6**, 3876–3882.
- Flory, P. J. [1953] *Principles of Polymer Chemistry* (Cornell University Press, Ithaca, NY).
- Galaev, I. and Mattiasson, B. [1999] “‘Smart’ polymers and what they could do in biotechnology and medicine,” *Trends in Biotechnol.* **17**(8), 335–340.
- Gent, A. N. and Cho, I. S. [1999] “Surface instabilities in compressed or bent rubber blocks,” *Rubber Chemistry and Technology* **72**, 253–262.
- Glangchai, L. C., Moore, M. C., Shi, L. and Roy, K. [2008] “Nanoimprint lithography based fabrication of shape-specific, enzymatically-triggered smart nanoparticles,” *J. Controlled Release* **125**, 263.
- Guvendiren, M., Yang, S. and Burdick, J. [2009] “Swelling-induced surface patterns in hydrogels with gradient crosslinking density,” *Advanced Functional Materials* **19**(19), 3038–3045.

- Guvendiren, M., Burdick, J. and Yang, S. [2010] “Kinetic study of swelling-induced surface pattern formation and ordering in hydrogel films with depth-wise crosslinking gradient,” *Soft Matter* **6**(9), 2044–2049.
- Hong, W., Zhao, X., Zhou, J. and Suo, Z. [2008] “A theory of coupled diffusion and large deformation in polymeric gels,” *Journal of the Mechanics and Physics of Solids* **56**, 1779–1793.
- Hong, W., Liu, Z. and Suo, Z. [2009a] “Inhomogeneous swelling of a gel in equilibrium with a solvent and mechanical load,” *International Journal of Solids and Structures* **46**, 3282–3289.
- Hong, W., Zhao, X. and Suo, Z. [2009b] “Formation of creases on the surfaces of elastomers and gels,” *Applied Physics Letters* **95**, 111901.
- Jeong, B., Bae, Y., Lee, D. and Kim, S. [1997] “Biodegradable block copolymers as injectable drug-delivery systems,” *Nature* **388**(6645), 860–862.
- Kang, M. K. and Huang, R. [2010a] “A variational approach and finite element implementation for swelling of polymeric hydrogels under geometric constraints,” *Journal of Applied Mechanics* **77**, 061004 (2010).
- Kang, M. K. and Huang, R. [2010b] “Swell-induced surface instability of confined hydrogel layers on substrates,” *Journal of the Mechanics and Physics of Solids* **58**, 1582–1598.
- Kang, M. K. and Huang, R. [2010c] “Effect of surface tension on swell-induced surface instability of substrate-confined hydrogel layers,” *Soft Matter* **6**, 5736–5742.
- Liu, Z., Hong, W., Suo, Z., Swaddiwudhipong, S. and Zhang, Y. [2010] “Modeling and simulation of buckling of polymeric membrane thin film gel,” *Computational Materials Science* **49**, S60–S64.
- Mora, T. and Boudaoud, A. [2006] “Buckling of swelling gels,” *Eur. Phys. J. E* **20**, 119–124.
- Peppas, N., Hilt, J., Khademhosseini, A. and Langer, R. [2006] “Hydrogels in biology and medicine: From molecular principles to bionanotechnology,” *Advanced Materials* **18**(11), 1345–1360.
- Qiu, Y. and Park, K. [2001] “Environment-sensitive hydrogels for drug delivery,” *Advanced Drug Delivery Reviews* **53**(3), 321–339.
- Sidorenko, A., Krupenkin, T., Taylor, A., Fratzl, P. and Aizenberg, J. [2007] “Reversible switching of hydrogel-actuated nanostructures into complex micropatterns,” *Science* **315**(5811), 487–490.
- Southern, E. and Thomas, A. [1965] “Effect of constraints on the equilibrium swelling of rubber vulcanizates,” *Journal of Polymer Science Part A General Papers* **3**(2), 641–646.
- Sultan, E. and Boudaoud, A. [2008] “The buckling of a swollen thin gel layer bound to a compliant substrate,” *Journal of Applied Mechanics* **75**, 051002.
- Tanaka, H., Tomita, H., Takasu, A., Hayashi, T. and Nishi, T. [1992] “Morphological and kinetic evolution of surface patterns in gels during the swelling process: Evidence of dynamic pattern ordering,” *Physical Review Letters* **68**(18), 2794–2797.
- Tanaka, T., Sun, S., Hirokawa, Y., Katayama, S., Kucera, J., Hirose, Y. and Amiya, T. [1987] “Mechanical instability of gels at the phase transition,” *Nature* **325**, 796–798.
- Tirumala, V., Divan, R., Ocola, L. and Mancini, D. [2005] “Direct-write e-beam patterning of stimuli-responsive hydrogel nanostructures,” *Journal of Vacuum Science and Technology B: Microelectronics and Nanometer Structures* **23**, 3124–3128.
- Tokarev, I. and Minko, S. [2009] “Stimuli-responsive hydrogel thin films,” *Soft Matter* **5**(3), 511–524.

- Treloar, L. R. G. [1975] “The physics of rubber elasticity,” *Oxford University Press, Oxford*.
- Trujillo, V., Kim, J. and Hayward, R. [2008] “Creasing instability of surface-attached hydrogels,” *Soft Matter* **4**(3), 564–569.
- Ulijn, R., Bibi, N., Jayawarna, V., Thornton, P., Todd, S., Mart, R., Smith, A. and Gough, J. [2007] “Bioresponsive hydrogels,” *Materials Today* **10**(4), 40–48.